Design and Optimization of a 8kW Linear Generator for a Direct-Drive Point Absorber

Jaeseung Kim, Jung Yoon Kim and Jin Bae Park
School of Electrical and
Electronic Engineering
Yonsei University
Seoul, Korea 120-749
Email: spctjs@gmail.com, kjy2587@gmail.com, jbpark@yonsei.ac.kr

***Abstract*—In this paper, a design and an optimization process of a linear generator for a wave energy converter (WEC) are studied. The linear generator is a crucial factor in planning a point absorber type WEC because of its vertical linear motion. Firstly, to design an adqeuate generator for the WEC, the generator force and the voltage equation are analyzed to derive the required magnetic flux, the thrust force and the current. Then, the stator core structure for satisfying those parameters are determined and an initial model is established. A finite element analysis (FEA) is conducted to verify the performance of the initial model. To improve the voltage distortion and reduce the detent force and the weight of the translator, a response surface optimization is applied. The optimal model's improvements are compared with the initial model for proving the feasibility of the overall process.**

I. INTRODUCTION

About 1TW of power is estimated as worldwide wave energy potential in which only the costal waves are included and over 10TW is considered if we even consider the waves in the far oceans [1]. This amount of renewable energy potential is comparable to the potential of the wind energy and the solar energy. Further, consistency and high energy density are notable properties of the wave energy [2]. For harnessing such advantageous wave energy, many challenges had been tried as forms of patents and research papers dealing how to capture the wave energy, but those trials had not been able to reach the commercialized level because there didn't exist heavy equipment vehicles for the ocean plant construction. However, the decreased unit cost of extracting the ocean energy caused by the matured construction and design technology made WECs get massive investment and be installed in several sites [3].

One of the most famous WEC is the PowerBouy developed by the Ocean Power Technologies [4]. It is a typical type of point absorber (PA) because the WEC acts as a floating point on a sea surface as shown in Fig. 1. This WEC absorbs the ocean waves as a form of vertical motion called heave which is induced by not only the waves but mechanical restraints. Since this machine utilizes the linear motion, the linear generator is inevitable choice for efficient operating.

Another famous WEC utilizing the heave motion is the Archimedes Wave Swing (AWS) installed on the seabed near Portugal [5], [6]. It is a submerged type as shown in Fig. 1 and consist of a oscillating cylinder lid and a silo comprising a linear generator and other miscellaneous mechanical parts.

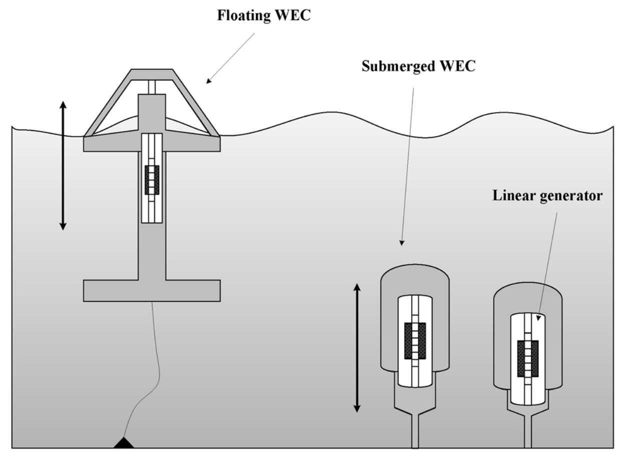

Fig. 1. Floating WEC and Submerged WEC equipping the linear generator.

Since it harnesses the heave motion and also adopts the direct-drive structure, the linear generator is strongly necessary.

To make those WECs above extract the maximum power from the incident waves, a resonance condition and a damping condition must be satisfied [7]. The resonance condition means that the frequency of the incident wave and the natural frequency of the oscillating body need to be same for absorbing maximum power. It is a problem of hydrodynamics of the oscillating body which highly affect the natural frequency of the body. Also, the damping condition means that the hydrodynamic damping coefficient should be equal to the damping coefficient from the generator. The damping force from the generator is mainly associated with the generator machine structure and the external load. In other words, to satisfy this condition, the generator and the load must be considered along with the hydrodynamic characteristics of the oscillating body.

However, unlike regular electric machinery with rotational generators, linear generators are installed in the PA type WECs. The requirement of the robust gearbox which does not need frequent maintanance makes the rotational generator not chosen as a proper energy conversion device for the PA type WECs. Also, the adoption of the direct-drive structure which decreases the mechanical loss makes the linear generator adequate for the PA, not the rotational generator. Therefore, the design of the linear generator optimized to the given wave

978-0-933957-40-4 ©2013 MTS

conditions and a power take-off system structure become a crucial step for planning a PA WEC project.

In this paper, the design and the optimization processes for the linear generator which fits the given operating environment are described. To follow those steps, a 8kW linear generator is projected to be designed. Firstly, the relationship between the output power, the generator speed and the generator thrust force is analyzed. Then, a stator structure and a magnet structure are considered to induce desired magnetic flux in the flux path. The magnetic circuit of the derived stator structure is studied and used to build the initial model for the finite element analysis. Finally, the response surface optimization is conducted to obtain the optimized model and by comparing it with the initial one, the validity of the entire process is proven.

II. Generator Design Study

The design process of the linear generator starts from determining the output power and the operating speed of the generator translator. This gives required thrust force and the amount of the magnetic flux inside the core. To induce the calculated magnetic flux in the stator, the number of slots and poles combinations has to be considered and this step is also crucial for the smooth motion of the translator. Then, from the magnetic circuit analysis, the rough model for the FEA can be established. Finally, based on the initial generator model, optimization technique is applied to fit the generator to the objective.

A. Basic Generator Equations

The induced voltage and the thrust force of the rotational generator can be deduced from Faraday's law and Lorentz force, respectively. Faraday's law and Lorentz force are defined as follows:

$$\varepsilon = -\frac{d\Phi}{dt}, \quad (1)$$

$$F = e(E + v \times B), \quad (2)$$

where, ε is the induced voltage, Φ is the flux linkage and F is the force acting on a particle of electric charge e with velocity of v, caused by an electric field E and a magnetic field B. From those equations, the generator terminal voltage (E_A) and the thrust force (F) can be derived, i.e.,

$$E_A = k_v \phi \omega, \quad (3)$$

$$F = k_f \phi I, \quad (4)$$

where k_v is the voltage constant including the stator construction characteristic such as the winding method and the dimensions of stator, ϕ is the flux linkage in the stator coils, ω is the mechanical angular velocity of the rotor, k_f is the force constant similar to the voltage constant and I is the current inside the generator [8].

However, since (3) is expressed for the rotational machine, converting to the linear one is required and it can be simply done by substituting the rotational velocity to the linear velocity. To obtain power equation using (3) and (4), a product of the generator voltage and the current or a product of the generator force and the velocity can be used. Therefore, the generator output power can be expressed as

$$P = k' \phi \omega I, \quad (5)$$

where k' is the machine construction constant including both k_v and k_f. Typically, the wave states, such as the period and the wavelength, near the WEC's operating site, are known before designing the generator and so the possible energy extraction is. Therefore, for designing a suitable linear generator for a certain location, we can calculate the required flux linkage and the machine construction constant.

In this paper, we plan to design the 8kW permanent magnet linear generator whose operating speed is 0.7m/s and rated voltage around 300V. This initial assumption make it possible to estimate the required flux, the current and the external thrust force.

TABLE I. Possible Combinations of Poles and slots

Slots	3	12	21	36	48
Poles	2	2	2	2	2
	4	**4**	**4**	4	4
		8	8	**6**	**8**
		10	**14**	**8**	10
		16	16	10	14
		...	...	...	...

B. Stator Structure

The number of slots per pole per phase q is one of the important parameters of characterizing the stator core. It denotes how many slots and magnetic poles exist in one stator core unit and is defined as

$$q = \frac{N_s}{N_p}, \quad (6)$$

where N_s is the number of slots in the core unit, and N_p is the number of magnetic poles under those slots.

In case of the q being integer, it is called an integral-slot structure. It has very high detent force because all slots has same mechanical degree to the nearest magnetic poles. Also, it has the poor output voltage shape because its flux linkage varies very rapidly along the stator motion direction. In contrast to the integral-slot structure, there exists a fractional-slot structure in which q is a fractional number. In this case, since the detent forces from each slot has different mechanical degrees and cancle out each other, the total detent force is very low. Also, the output voltage shape is very close to the sinusoidal wave of the fundamental frequency.

Common possible combinations of slots and poles for 3-phase machine are expressed in table I, but there still exist numerous combinations which are not shown here, for more combinations, see [9]. Especially, combinations which minimize the detent force are written in boldface such as 3-slot 4-pole and 21-slot 4-pole combinations.

In case of the application of the WECs equipping the linear generator, low detent force is desired because the WECs have zero speed periodically and the detent force acts as an obstruction in the low speed region. Also, large number of

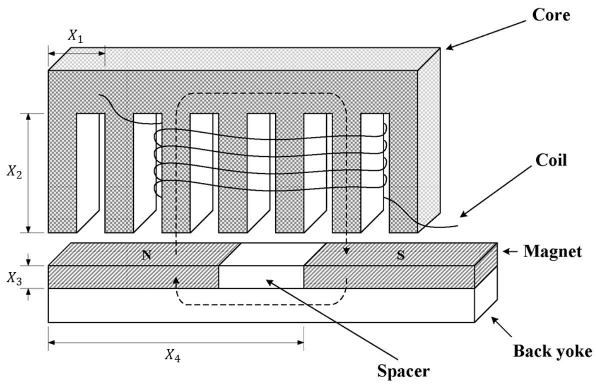

Fig. 2. The generator diagram and its one possible flux path.

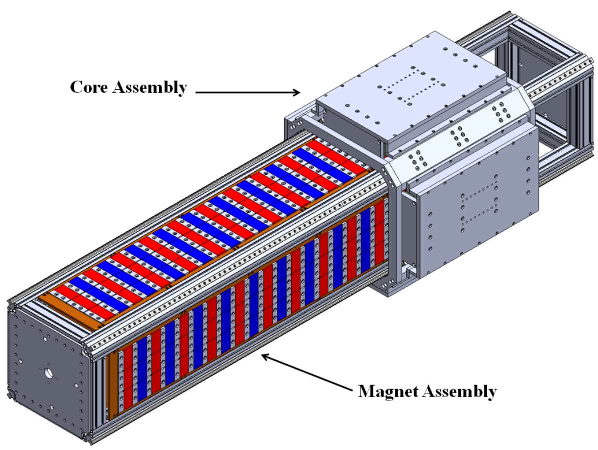

Fig. 3. The generator rendering image.

poles is required for shaping sinusoidal voltage output in the low speed region around the translator's return position.

After comparing the above combinations, we chose 36-slot 8-pole model since it has better performance in terms of the detent force and the voltage output shape. The determined stator structure is shown in Fig. 2. Also, to scale the output power by four and increase the space efficiency, the structure is configured as 4 side. As shown in Fig. 3, totally 4 cores are connected as to form the magnet assembly, and 4 magnet parts are connected as the magnet assembly. Each side would make the quarter of the overall performance.

C. Magnetic Circuit Theory

After determining the stator structure such as slots per pole per phase, the next step for calculating the magnetic flux linkage is the magnetic circuit analysis. In the magnetic circuit analysis, we represent the possible flux path in the generator as a reluctance network and solve the network to estimate the flux linkage of the overall magnetic circuit. A magnet is expressed as a magnetomotive force (MMF) which is analogous to a voltage source in an electric circuit. A stator core, an air gap and a back yoke are represented as reluctances which affect as resistors in the electric circuit. The relation between the

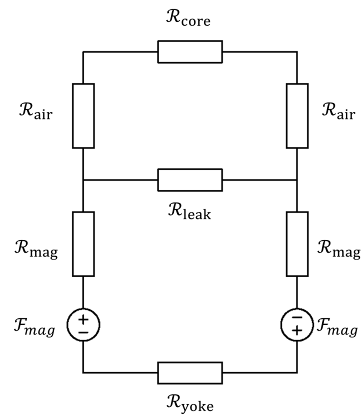

Fig. 4. The magnetic circuit of the possible flux path.

magnetomotive force $\mathcal{F}$, the reluctance $\mathcal{R}$ and the magnetic flux ϕ is expressed as follows:

$$\mathcal{F} = \mathcal{R}\phi. \tag{7}$$

It means that if we use the stronger and bigger magnet, or we shorten the air gap and any flux path, the overall magnetic flux would increase.

One of the possible flux path of the determined generator structure is indicated as a dashed line in Fig. 2. The flux is generated from the one magnet and passes through the airgap. Then, most of the flux pass inside the core toward another pole. However, at the same time, the flux can go from one magnet to another directly and it is regarded as a leakage flux. The analyzed flux path can be expressed as the magnetic circuit. The air gap, the steel core, the back yoke and the magnets are converted into adequate magnetic circuit elements, for example, the magnet is expressed as a combination of a magnetomotive force and a reluctance. The equivalent magnetic circuit of above flux path is shown in Fig. 4. Solving the reluctance network, the flux passing through the stator coil can be obtained and considering the number of coil turns, the flux linkage in (5) can be calculated.

D. Finite Element Method Design

The magnetic circuit analysis method described above gives a feasible result of magnetic flux, but this process necessarily requires to include possible flux leakages. Some of common flux leakage reluctances are already derived in [10]. However, most leakages are hard to be anticipated and calculated, because lots of commercial generators have very complex shapes to analyze using Maxwell's equations. Therfore, a lot of generator design is acheived by the FEA because it can compute the performance of the design and its losses. Also, quick design adjustment is another advantage of the FEA based design. However, both methods are not exclusive but complementary because, from the magnetic circuit, the structural characteristic such as q or several major leakages can be analyzed quickly, and the derived parameters help to establish and to simulate the design in the FEA stage.

To design 8kW linear generator, the q value and the flux linkage derived in the previous stage are used to determine

TABLE II. THE SPECIFICATION OF THE INITIAL MODEL

Rated power per side	2.0kW
Rated voltage per phase	300V
Rated current per phase	5A
Operating speed	0.7m/s
Number of coil turns	100
Air gap lengths	4mm
Magnet dimensions	300mm × 60mm × 8mm
Core dimensions	300mm × 722mm × 150mm
Pole Pitch	90mm
Slot Pitch	20mm
Weight	160.5kg

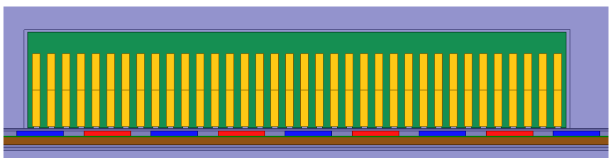

Fig. 5. The 36-slot 8-pole model for the finite element analysis.

the initial model of the FEA. It consists of 4 sides of cores and those cores are externally connected. Eash side has to be capable of 2kW of output. We decided to make that the projected linear generator's no-load output voltage has to be above 300V and the output power to be around 2kW from each side. The determined dimensions and specifications are shown in table II and its FEA model is shown in Fig. 5.

The output no-load voltage of the initial model is shown in Fig. 6. The three phases of voltages are generated above 300V and it should have more than 10% of the desired voltage output under the load condition because of the armature reaction and some other leakages. Also, to be able to supply generated electricity to the power grid, the low total harmonic distortion (THD) of the output voltage is recommeneded, so decreasing THD would be covered in the optimizing stage. The detent force acting on the stator is shown in Fig. 7. The peak detent force is 483N and it still acts as a periodic force even though it has the fractional-slot structure which can be overcome by adopting the skewed magnets and the rounded core ends. However, lowering the detent force by not adjusting the overall structure but slightly changing design parameters would be tried in the optimization stage.

III. RESPONSE SURFACE OPTIMIZATION

A. Response Surface Method

The response surface analysis is a method as one of the design of experiment method using a regression analysis, to analyze the natural phenomena represented by the value referred as responses. The input variables are the factors which affect on responses that are adjusted by the experimenter. This method can be applied to search for the argument condition for the optimum value or to determine the change in responses due to factors. When the response is η, the function f of coded independent variables x_1,x_2,$\cdots$ are expressed as follows:

$$\eta = f(x_1, x_2, \cdots) + \epsilon, \tag{8}$$

where ϵ is an error which is referred to a residual. Since the real response function cannot be represented to a formula, it is

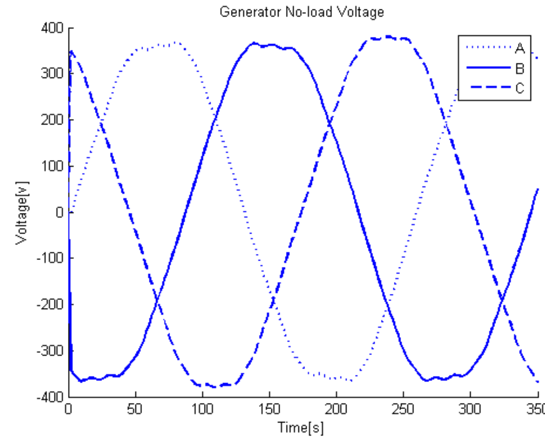

Fig. 6. The no-load voltage of the initial model.

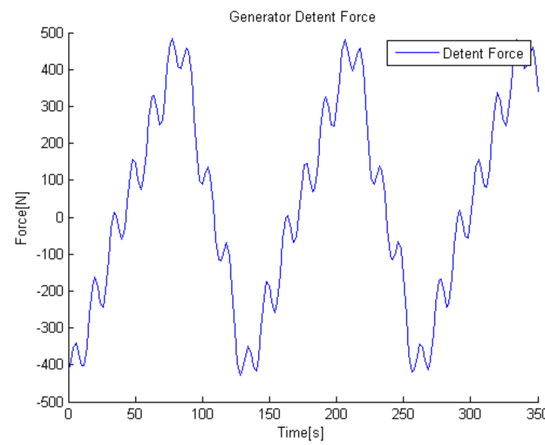

Fig. 7. The detent force of the initial model.

necessary to use an approximated model. Usually, low order polynomial such as 1st order or 2nd order, is used. In the case of searching the optimal point, the response surface is assumed to be curved shape, and the 2nd order model is used [11]. In order to approximate a curved surface, the three or more levels for each factor must be measured. The most popular class of the 2nd order designs is the central composite design (CCD). Then, the most effective experimental design order is formed, and it can be configured an approximate expression to calculate the regression variables using the least square method. The constructed empirical model is as follows:

$$\eta = \beta_0 + \sum_{j=1}^{k} \beta_j x_j + \sum_{j=1}^{k} \beta_{jj} x_j^2 + \sum_{i,j}^{k} \beta_{ij} x_i x_j, \tag{9}$$

where β_0, β_j, β_{jj} and β_{ij} are the regression coefficients. In this paper, using the response surface method (RSM), while satisfying the constraints, finding factors to show the performance of the optimal generator is tried.

B. Setting of the Empirical Response Surface

Let X_1 (Slot pitch), X_2 (Slot height), X_3 (magnet height) and X_4 (magnet width ratio) be selected in the four arguments

TABLE III. EXPERIMENTS RESULTS

Exp.	X_1	X_2	X_3	X_4	Y_1	Y_2	Y_3
1	18	70	6	0.6	342.632	102.181	8.127
2	22	70	6	0.6	375.379	130.146	11.186
3	18	90	6	0.6	324.914	117.046	8.665
4	22	90	6	0.6	372.095	148.295	11.204
5	18	70	10	0.6	517.210	108.223	7.308
6	22	70	10	0.6	570.716	137.531	9.183
7	18	90	10	0.6	538.190	123.089	8.718
8	22	90	10	0.6	557.992	155.680	11.486
9	18	70	6	0.73	366.757	102.134	6.142
10	22	70	6	0.73	444.175	130.088	6.249
11	18	90	6	0.73	363.078	116.999	5.334
12	22	90	6	0.73	418.624	148.237	6.246
13	18	70	10	0.73	596.422	108.145	6.795
14	22	70	10	0.73	691.155	137.435	5.287
15	18	90	10	0.73	556.231	123.010	5.983
16	22	90	10	0.73	724.204	155.584	4.740
17	16	80	8	0.665	509.894	98.207	7.041
18	24	80	8	0.665	574.824	158.749	6.214
19	20	60	8	0.665	463.489	110.986	1.138
20	20	100	8	0.665	481.904	144.000	5.395
21	20	80	4	0.665	238.599	120.796	4.893
22	20	80	12	0.665	677.111	134.189	4.225
23	20	80	8	0.535	474.764	127.562	15.381
24	20	80	8	0.795	481.098	127.423	10.270
25	20	80	8	0.665	473.801	127.493	3.804
26	20	80	8	0.665	473.801	127.493	3.804
27	20	80	8	0.665	473.801	127.493	3.804
28	20	80	8	0.665	473.801	127.493	3.804
29	20	80	8	0.665	473.801	127.493	3.804
30	20	80	8	0.665	473.801	127.493	3.804
31	20	80	8	0.665	473.801	127.493	3.804

that have a major impact on the performance of the linear generator. Y_1 (detent force), Y_2 (weight) and Y_3 (THD) are set as the objective functions which are typical parameters showing the performance of the generator.

The experimental order by using CCD with divided into three levels (-1, 0, 1) of variables and the responses obtained using FEM are shown in table III. The obtained empirical models of respective objective functions are as follows

$$\begin{aligned} Y_1 = {} & 473.801 + 32.738X_1 - 0.512X_2 + 109.23X_3 \\ & + 24.92X_4 + 22.256X_1^2 - 1.844X_2^2 \\ & - 5.555X_3^2 - 0.536X_4^2 + 2.006X_1X_2 \\ & + 7.695X_1X_3 + 15.152X_1X_4 + 3.209X_2X_3 \\ & - 1.477X_2X_4 + 12.893X_3X_4, \end{aligned} \tag{10}$$

$$\begin{aligned} Y_2 = {} & 127.493 + 15.136X_1 + 8.254X_2 \\ & + 3.348X_3 - 0.035X_4 + 0.246X_1^2 \\ & + 0.821X_1X_2 + 0.335X_1X_3 - 0.003X_1X_4 \\ & - 0.009X_3X_4, \end{aligned} \tag{11}$$

$$\begin{aligned} Y_3 = {} & 3.804 + 0.595X_1 + 0.442X_2 \\ & - 0.208X_3 - 1.638X_4 + 1.234X_1^2 \\ & - 0.071X_2^2 + 0.253X_3^2 + 2.319X_4^2 \\ & + 0.090X_1X_2 - 0.295X_1X_3 - 0.748X_1X_4 \\ & + 0.163X_2X_3 - 0.402X_2X_4 + 0.083X_3X_4. \end{aligned} \tag{12}$$

TABLE IV. THE SPECIFICATION OF THE OPTIMIZED MODEL

Rated power per side	2.0kW
Rated phase voltage	300V
Rated phase current	5A
Operating speed	0.7m/s
Number of coil turns	100
Air gap lengths	4mm
Magnet dimensions	300 mm × 58.59 mm × 7 mm
Core dimensions	300 mm × 671.6 mm × 118.95 mm
Pole Pitch	83.7 mm
Slot Pitch	18.6 mm
Weight	123.13kg

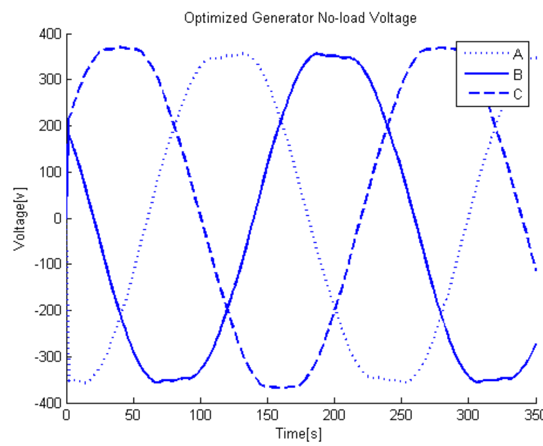

Fig. 8. The no-load voltage of the optimized generator.

The R^2 of each model, a measure of the amount of reduction in the variability of Y obtained by using the regressor variables in the model for the Y_1, Y_2 and Y_3 are 100%, 97.11% and 96.80%, respectively. Since the R^2 always increases as terms are added to the model, R^2_{adj} is preferred to estimate the validity. It is an index that considering whole X as well as the effect of X itself and their values for each objective functions are Y_1(100%), Y_2(94.40%), Y_3(93.82%). Therefore, it shows that the empirical model is properly fitted.

C. Optimization of the Response Surface with constraints

Having rated power conditions, the constraints of the three objective functions are set to $400 < Y_1 < 460$, $120 < Y_2 < 127$ and $4 < Y_3 < 6$. The detent force is the most critical factor in the performance of the linear generator. Thus, the weight of (Y_1:Y_2:Y_3=3:1:1) is applied when combining those objective functions. Once the rated power is ensured, it is necessary to lighten the weight for the efficiency of the overall system. The constraint boundaries are chosen taking into account the means of the data. Also, when the voltage waveform is closer to a sinusoidal wave, the control characteristic would be better, and for the power grid connection, low THD is recommended.

D. Result

The specification of the derived optimum model is shown in table IV. The FEA is conducted again to confirm the expected data from the RSM. The no-load terminal voltage is shown in Fig. 8. It shows improved THD characteristics because of the

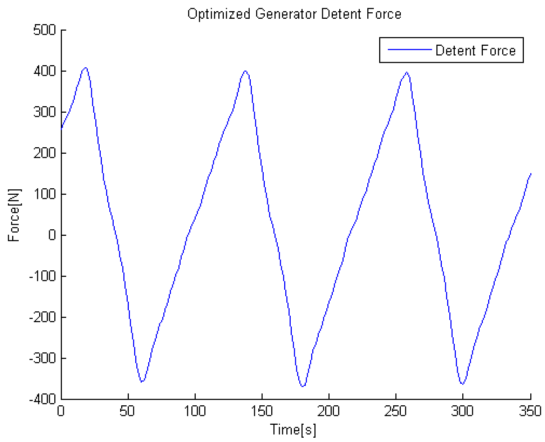

Fig. 9. The detent force of the optimized stator.

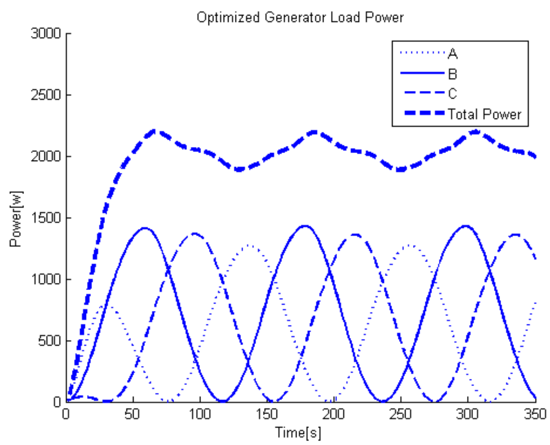

Fig. 10. The generated power of the optmized generator

TABLE V. PERFORMANCE COMPARISON ALONG THE DESIGN STEPS

Parameter	Initial Design	RSM Predicted	FEM Optimum
F_d	483N	400.08N	407N
Weight	160.5kg	122.98kg	123.1kg
THD	4.133	4.55	5.740

objective function for the THD and still maintains the level of voltage as we induced in previous stages. The detent force of the optimum model is shown in Fig. 9. The maximum of the detent force is drastically reduced, comparing to Fig. 7. The left periodic detent force can be reduced if we increase the weight of the detent force in the objective function or adopt another unique structure as described above. The generated power from the optimum design is shown in Fig. 10. Its total power from 3 phases are fluctuating around 2000W as we originally expected. The power ripple can be improved by adjusting coil turns at the end slots but it is not dealt here. From this result, we can conclude that the designed linear generator is satisfying the rated power of 2kW per side and 8kW totally.

The initial model, the optimal model estimated by the RSM and the FEA are shown on table V for verifying the optimization technique. Above all, the detent force decreased by 17.2%. Weight is also reduced significantly than the initial model, because the size of the slots and the magnets decreased. As the proportion of the magnet is increased in the pole pitch, there exists a change in the THD. Although the THD was slightly larger than the initial model, since the impact to the performance is smaller than the weight and the detent force, the effect of this rise can be ignored.

IV. Conclusion

In this paper, the design and the optimization processes of the 8kW linear generator for WEC was studied. To estimate the required flux amount, the generator force equation and the voltage equation was accounted. The detent force minimizing structure and its magnetic circuit was analyzed to choose the suitable stator structure. The FEA was used to verify the iniatial design and response surface optimization. Finally, by comparing the initial model with the optimized one, the validity of the design process and the response surface method was shown.

Acknowledgment

This work was supported by the New & Renewable Energy of the Korea Institute of Energy Technology Evaluation and Planning (20103020070070) grant funded by the Korea government Ministry of Knowledge Economy.

References

[1] N. N. Panicker, “Power resource potential of ocean survace waves,” *Proceedings of the wave and salinity gradient workshop*, 1976, pp. J1-J48.

[2] M. Leijon, H. Bernhoff, M. Berg and O. Agren, “Economical considerations of renewable electric energy production especially development of wave energy,” *Renewable Energy*, vol. 28, no. 8, pp. 1201-1209, July 2003.

[3] A. Clement, P. M. Cullen, A. Falcao, A. Fiorentino, F. Garener, K. Hammarlund, G. Lemonis, T. Lewis, K. Nielsen, S. Petroncini, M. Pontes, P. Schild, B. Sjostrom, H. Sorensen and T. Thrope, “Wave energy in Europe: current status and perspectives,” *Renewable and Sustainable Energy Rev.*, vol. 6, no. 5, pp. 405-453, Oct.2002.

[4] A. Westwood, “Wave and tidal project review,” *Renewable Energy Focus*, vol. 8, no. 4, pp. 30-33, Jul. 2007.

[5] AWS Ocean Energy, www.awsocean.com.

[6] H. Polinder, M. E. C. Damen and F. Gardner, “Linear PM generator system for wave energy conversion in the AWS,” *IEEE trans. on Energy Conversion*, vol. 19, no. 3, pp. 583-589, Sep. 2004.

[7] F. Wu, X. P. Zhang, P. Ju and M. J. H. Sterling, “Modeling and control of AWS-based wave energy conversion system integrated into power grid,” *IEEE trans. on. Power systems*, vol. 23, no. 3, pp. 1196-1204, Aug. 2008.

[8] S. J. Chapman, *Electric Machinery Fundamentals*, McGraw Hill 2004.

[9] J. R. Hendershot and T. J. E. Miller, *Design of Brushless Permanent-Magnet Motors*, Oxford University Press, 1955.

[10] M. F. Hsieh and Y. C. Hsu, “A generalized magnetic circuit modeling approach for design of surface permanent-magnet machines,” *IEEE Trans. on Ind. Electro.*, vol. 59, no. 2, pp. 779-792, Feb. 2012.

[11] H. M. Hasanien, A. S. Abd-Rabou and S. M. Sakr, “Design optimization of transverse flux linear motor for weight reduction and performance improvement using response surface methodology and genetic algorithms,” *IEEE trans. on. Energy conversion*, vol. 25, no. 3, Sep. 2010.

[12] D.K. Hong, B.C.Woo, D.H. Koo and D.H. Kang, “Optimum design of transverse flux linear motor for weight reduction and improvement thrust force using response surface methodology,” *IEEE Trans. Magn.*, vol. 44, no. 11, pp. 4317-4320, Nov. 2008.